

## Force-velocity relations of rat cardiac myosin isozymes sliding on algal cell actin cables in vitro

Seiryō Sugiura <sup>a,\*</sup>, Hiroshi Yamashita <sup>a</sup>, Masataka Sata <sup>a</sup>, Shin-ichi Momomura <sup>a</sup>,  
Takashi Serizawa <sup>a</sup>, Kazuhiro Oiwa <sup>b</sup>, Shigeru Chaen <sup>b</sup>, Teruo Shimmen <sup>c</sup>, Haruo Sugi <sup>b</sup>

<sup>a</sup> Second Department of Internal Medicine, School of Medicine, University of Tokyo, 7-3-1 Hongo, Bunkyo-ku, Tokyo 113, Japan

<sup>b</sup> Department of Physiology, School of Medicine, Teikyo University, Itabashi-ku, Tokyo 173, Japan

<sup>c</sup> Department of Life Science, School of Science, Himeji Institute of Technology, Kamigori-gun, Hyogo-ken 678-2, Japan

Received 18 January 1995; accepted 3 April 1995

---

### Abstract

The difference in kinetic properties between two myosin isozymes ( $V_1$  and  $V_3$ ) in rat ventricular myocardium was studied by determining the steady-state force-velocity ( $P$ - $V$ ) relations in the ATP-dependent movement of  $V_1$  and  $V_3$ -coated polystyrene beads on actin cables of giant algal cells mounted on a centrifuge microscope. The maximum unloaded velocity of bead movement was larger for  $V_1$  than for  $V_3$ . The velocity of bead movement decreased with increasing external load applied by the centrifuge microscope, and eventually reached zero when the load was equal to the maximum isometric force ( $P_0$ ) generated by the myosin heads. The maximum isometric force  $P_0$  was less than 10 pN, and did not differ significantly between  $V_1$  and  $V_3$ . The  $P$ - $V$  curves consisted of a hyperbolic part in the low force range and a non-hyperbolic part in the high force range. The critical force above which the curve deviated from the hyperbola was much smaller for  $V_1$  than for  $V_3$ . An analysis using a model with an extremely small number of myosin heads involved in the bead movement suggested a marked difference in kinetic properties between  $V_1$  and  $V_3$ .

**Keywords:** Cardiac myosin; Motility assay, in vitro; Centrifuge microscope; Force-velocity relation; Myosin

---

### 1. Introduction

Mammalian ventricular myocardium can contain three different myosin isozymes,  $V_1$ ,  $V_2$  and  $V_3$ , which are distinguished from each other by their heavy chain components.  $V_1$  and  $V_3$  are homodimers of  $\alpha$ - and  $\beta$ -heavy chains, respectively, while  $V_2$  is a heterodimer of  $\alpha$ - and  $\beta$ -heavy chains [1]. Relative amounts of these myosin isozymes in the myocardium change under a variety of conditions such as ageing, pressure overload, thyroid dysfunction and malnutrition [2,3], constituting the mechanism of cardiac adaptation processes, especially in small animals. Although there is a correlation between the maximum shortening velocity of cardiac muscle preparation and its isozyme distribution and ATPase activity [4,5], complex structure of the preparation together with a number of factors affecting contractile activity make it difficult to determine to what extent the change in the shortening

velocity originates from the change in myosin isozyme distribution per se.

Recent development of in vitro motility assay systems has made it possible to study ATP-dependent sliding between actin and myosin without complications arising from intact muscle preparations. Using an assay system in which myosin-coated latex beads are made to slide on well organized actin filament arrays (actin cables) of giant algal cells [6], Sugiura and co-workers found that both unloaded bead sliding velocity and ATPase activity of rabbit cardiac myosin correlate well with its myosin isozyme distribution [7,8], indicating that the change in unloaded actin-myosin sliding velocity actually reflects myosin isozyme distribution.

The purpose of the present work is two-fold; first, to determine the difference in kinetic properties between the two myosin isozymes,  $V_1$  and  $V_3$ , in more detail by determining their force-velocity ( $P$ - $V$ ) relations with an in vitro assay system, in which myosin-coated polystyrene beads are made to slide on actin cables in giant algal cell preparations mounted on a centrifuge microscope to apply

---

\* Corresponding author. Fax: +81 3 38140021.

external loads on the beads [9], and secondly to give a possible explanation for the obtained  $P$ - $V$  relations of in vitro actin-myosin sliding, which only involves an extremely limited number of myosin molecules and differs markedly from the hyperbolic  $P$ - $V$  relations of contracting muscle. It will be shown that the marked deviation from the hyperbola of the  $P$ - $V$  curves obtained can be explained, on the basis of the Huxley contraction model [10], as being due to the extremely small number of myosin heads involved. On this basis, the different  $P$ - $V$  curves between  $V_1$  and  $V_3$  results from different turnover rate of actin-myosin interaction between  $V_1$  and  $V_3$ .

## 2. Methods

### 2.1. Preparation of myosin samples

Myosin samples consisting predominantly of  $V_1$  were obtained from 3-week-old Wistar rats (body weight 50–70 g), while those predominantly containing  $V_3$  were obtained from 10-week-old rats (body weight 250–300 g), in which hypothyroidism had been induced by adding 1-methyl-2-mercaptoimidazol (Methimazole, Chugai Pharmaceutical Co., Japan) to drinking water for 10 weeks, the average daily dose of Methimazole being 15 mg. Hearts were excised from the animals under diethyl ether anaesthesia, and myosin samples were prepared from the ventricular myocardium by the method of Katz et al. [11] with slight modifications. All procedures were carried out at 4°C, in the presence of 5 mM dithiothreitol and  $5 \cdot 10^{-6}$  mg/ml leupeptin (proteinase inhibitor). At the final stage, actin was removed from the sample by centrifugation ( $100\,000 \times g$  for 3 h). Protein concentration of both  $V_1$  and  $V_3$  samples were adjusted to 1.9 g/l to be used for the in vitro assay experiments.

### 2.2. Biochemical assays

Myosin isozyme contents in the samples were determined by pyrophosphate polyacrylamide gel electrophoresis at 3°C using a Pharmacia GE4 electrophoresis chamber [12]. Gels were fixed and stained with Coomassie brilliant blue and scanned by a densitometer (LKB 2202, LKB Produkter, Sweden) at 600 nm.  $\text{Ca}^{2+}$ -activated ATPase activity was determined by measuring inorganic phosphate ( $\text{P}_i$ ) liberation [13]. The reaction was run for 5 min (25°C, pH 7.5) in 50 mM Tris/1 mM ATP/10 mM  $\text{CaCl}_2$ . Protein concentration was determined by the method of Lowry et al. [14].

### 2.3. Preparation of myosin-coated beads

Tosyl-activated polystyrene beads (diameter 2.8  $\mu\text{m}$ ; specific gravity 1300  $\text{kg}/\text{m}^3$ , Dynal, Norway) were incubated in a 100 mM borate buffer (pH 9.5) containing 10

g/l poly(L-lysine) (Sigma) for 24 h, and then further incubated in  $V_1$  or  $V_3$  sample in 20 mM piperazine- $N,N'$ -bis(2-ethanesulfonic acid) (Pipes) (pH 7.0)/5 mM ethylene glycol bis( $\beta$ -aminoethyl ether)- $N,N,N',N'$ -tetraacetic acid (EGTA)/6 mM  $\text{MgCl}_2$ /200 mM sorbitol/50 mM KOH. The myosin-coated beads thus prepared were precipitated by centrifugation, and resuspended in 20 mM Pipes (pH 7.0)/5 mM EGTA/6 mM  $\text{MgCl}_2$ /1 mM ATP/200 mM sorbitol/50 mM KOH (MgATP solution).

### 2.4. Internodal cell preparation

Giant internodal cells (diameter, approx. 0.5 mm; length 12–17 cm) were isolated from the green alga *Nitellopsis obtusa*, and cut open at both ends, and the cell sap was replaced with MgATP solution by perfusing the cell interior with the solution several times the cell volume [15]. At the final stage of the perfusion, the myosin-coated polystyrene beads were introduced into the cell. Then, both ends of the cell were ligated with strips of polyester thread. The internodal cell preparation (diameter, approx. 0.5 mm; length, approx. 1 cm) was put into a centrifuge cuvette ( $33 \times 20 \times 3$  mm deep) filled with artificial pond water containing 0.1 mM each KCl, NaCl and  $\text{CaCl}_2$  (pH 5.6) [9].

### 2.5. Centrifuge microscope and video system

The centrifuge microscope consisted of a light microscope, a rotor (diameter, 16 cm) that could be rotated at 250–5000 rpm ( $(4\text{--}1900) \times g$ ), and a stroboscopic light source (xenon tube) as shown diagrammatically in Fig. 1. The xenon tube was triggered each time the internodal cell preparation came under the objective lens. The position of a metal piece at the rotor edge opposite the cuvette was sensed by a position sensor (light source-photodiode system) to result in generation of an electrical pulse, which was used to trigger the xenon tube and to be fed to a pulse

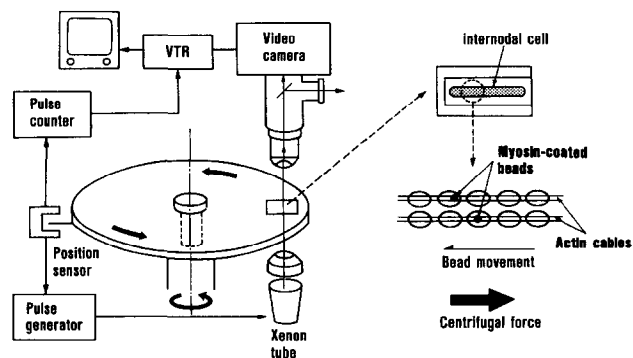


Fig. 1. Diagram of the experimental arrangement. The internodal cell preparation containing myosin-coated polystyrene bead is placed in the cuvette on the rotor of the centrifuge microscope. The beads moving on actin cables are subjected to centrifugal forces serving as external loads. For further explanation, see text.

counter monitoring the rate of rotation of the rotor. Thus, the stationary image of the preparation could be observed and recorded on videotape (30 frames/s) with a video camera (C-2847, Hamamatsu Photonics, Japan). Further details of the centrifuge microscope and the video system have been described elsewhere [9,16].

## 2.6. Experimental procedure

The internodal cell preparation containing the myosin-coated polystyrene beads was placed in the centrifuge cuvette in such a way that its chloroplast rows, along which actin cables ran straight, were parallel to the direction of centrifugal force. The bead moving on actin cables was observed with a  $40\times$  dry objective (n.a. 0.55) and recorded with a video cassette recorder (VO-9600, Sony, Japan), attention being focused only on the beads that moved smoothly over many seconds under various centrifugal forces. The amount of centrifugal force  $P$  serving as load on the bead is estimated by:

$$P = \Delta\rho \cdot V \cdot r \cdot \omega^2$$

where  $\Delta\rho$  is the difference in density between the bead and the surrounding medium ( $=0.3$ ),  $V$  is the bead volume ( $=12\ \mu\text{m}^3$ ),  $r$  is the effective radius of centrifugation, and  $\omega$  is the angular velocity of the rotor. The bead movement was analyzed on replay from the video cassette recorder, the change in the bead position being measured on the monitor screen ( $30\times 20\text{ cm}$ ; magnification  $2000\times$ ) with an accuracy of  $<0.5\ \mu\text{m}$  by a video microscaler (IV-500, For-A, Japan). All experiments were made at room temperature ( $20\text{--}23^\circ\text{C}$ ).

## 3. Results

### 3.1. Biochemical characterization of myosin samples

Pyrophosphate polyacrylamide gel electrophoretic patterns of two different myosin samples are shown in Fig. 2, together with their densitometric tracings. Each tracing

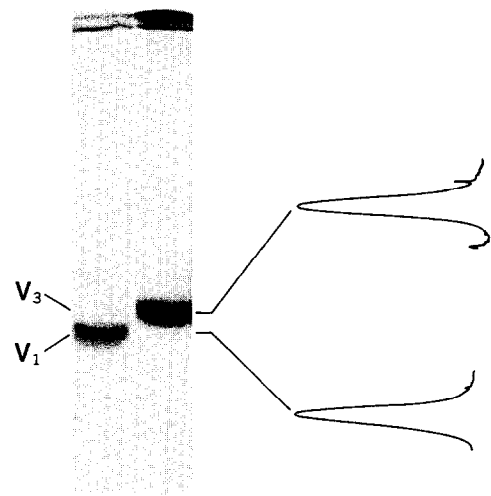


Fig. 2. Pyrophosphate polyacrylamide gel electrophoretic patterns of  $V_1$  and  $V_3$  samples (left) and their densitometric tracings (right).

shows a single peak, indicating that the myosin sample obtained from normal rats contained 100%  $V_1$  whereas the samples obtained from hypothyroid rats contained 100%  $V_3$ . This indicates that the beads incubated in the normal myosin sample are coated with  $V_1$  isozyme, while the beads incubated in the hypothyroid myosin are coated with  $V_3$  isozyme. In agreement with an earlier report [17], the normal ( $V_1$ ) and the hypothyroid ( $V_3$ ) myosin samples showed  $\text{Ca}^{2+}$ -activated ATPase activity of 1.11 and  $0.33\ \mu\text{mol P}_i/\text{mg per min}$ , respectively.

### 3.2. Movement of the myosin-coated beads on actin cables

In agreement with previous reports [6,9], the myosin-coated beads moved on actin cables in one direction determined by the polarity of actin cables. Without centrifugal forces, i.e., under the unloaded condition, both  $V_1$ - and  $V_3$ -coated beads moved with constant velocities. The maximum unloaded velocity of bead movement was significantly larger in  $V_1$ - than in  $V_3$ -coated beads, being  $1.70 \pm 0.62\ \mu\text{m/s}$  (mean  $\pm$  S.D.,  $n = 25$ ) for  $V_1$  and  $0.61$

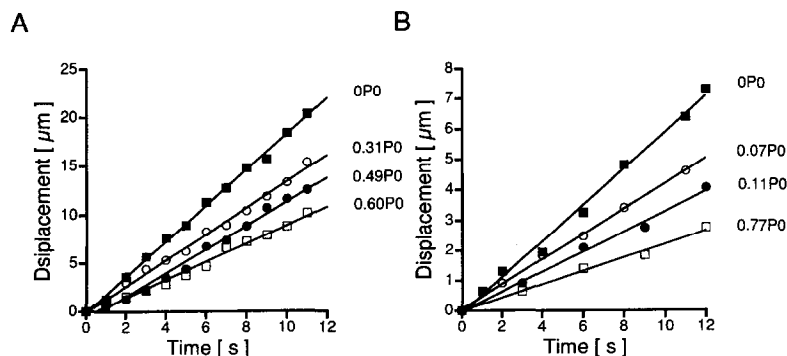


Fig. 3. Constant velocity movements of a myosin-coated bead on actin cables under different external loads expressed relative to  $P_0$ . Regression lines were drawn by the least-square method. (A) The beads coated with  $V_1$  and its  $P_0$  was  $5.6\ \text{pN}$ . (B) The bead was coated with  $V_3$  and its  $P_0$  was  $8.3\ \text{pN}$ .

$\pm 0.15 \mu\text{m/s}$  ( $n = 17$ ) for  $V_3$  ( $P < 0.05$ ). These values agree well with those obtained by Sugiura et al. [7].

When centrifugal forces directed opposite the bead movement were applied to the beads, their velocity of movement on actin cables decreased with increasing centrifugal forces serving as positive external loads. Fig. 3 shows a typical effect of external load on the velocity of  $V_1$ - and  $V_3$ -coated bead movement. As with beads coated with rabbit skeletal muscle myosin [9], both  $V_1$ - and  $V_3$ -coated beads moved with constant velocities under various external loads, indicating the presence of a steady-state relation between the force (= load) generated by the actin–myosin interaction and the velocity of the actin–myosin sliding. When the amount of external load became equal to the maximum isometric force ( $P_0$ ) generated by the myosin molecules interacting with actin cables, the bead stopped moving to stay at the same position for 5–10 s, and was then suddenly detached from actin cables to flow away in the direction of applied centrifugal force [9].

### 3.3. Difference in the steady-state $P$ - $V$ relation between $V_1$ - and $V_3$ -coated beads

We obtained the steady-state  $P$ - $V$  relation of  $V_1$ - and  $V_3$ -coated beads moving on actin cables by applying various loads on the beads. The procedure was, however, not easy for of the following reasons. First, we had to obtain reasonable number of data points for several different loads, including  $P_0$ . As the values of  $P_0$  differed from bead to bead and were therefore unpredictable at the start of each experiment to determine the  $P$ - $V$  relation for a particular bead, we frequently applied loads exceeding  $P_0$  to the beads to result in failure to obtain the whole  $P$ - $V$  curves. Secondly, as the accurate determination of  $P_0$  required many seconds; while the beads were moving on actin cables over long distances, the beads tended not to move smoothly during the course of experiment probably because actin cables were not entirely homogeneous over long distances.

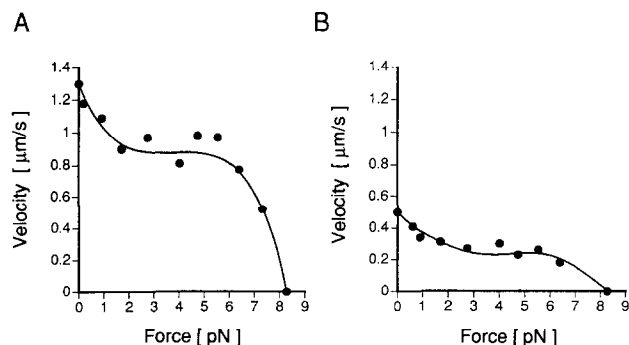


Fig. 4. Typical examples of the  $P$ - $V$  relation obtained from a  $V_1$ -coated (A) and that obtained from a  $V_3$ -coated bead (B). In both cases, the curve in the low force region was fitted to a hyperbola ( $a/P_0$  was  $-0.41$  in A and  $0.14$  in B) by the non-linear least-square method.

In spite of the difficulties stated above, we could obtain several complete  $P$ - $V$  curves for both  $V_1$ - and  $V_3$ -coated beads (see Fig. 4). Fig. 4 shows typical  $P$ - $V$  relations of  $V_1$ - and  $V_3$ -coated beads. As has been the case with beads coated with skeletal muscle myosin [9], the  $P$ - $V$  curves obtained consisted of hyperbolic part in the low force range and non-hyperbolic part in the high force range. In both  $V_1$ - and  $V_3$ -coated beads, the velocity of bead movement decreased to reach a plateau level when the load was increased from zero to a certain value, while further increase of the load to  $P_0$  produced a steep decrease of the velocity to zero. In contrast with the definite difference in the maximum unloaded velocity of bead movement between  $V_1$ - and  $V_3$ -coated beads, the value of  $P_0$  did not exceed 10 pN, and did not differ significantly between  $V_1$ - and  $V_3$ -coated beads, being  $7.0 \pm 3.7$  pN ( $n = 5$ ) for  $V_1$  and  $6.2 \pm 2.0$  pN ( $n = 5$ ) for  $V_3$ . Since the myosin concentration was the same between the  $V_1$  and the  $V_3$  samples in which the beads were incubated, this result may be taken to indicate that the value of  $P_0$  generated by each myosin head may be the same in both  $V_1$  and  $V_3$ . It should be noted that the isometric forces we measured were time averaged forces, but not peak transient forces that each myosin head generates while attached to actin. On this basis, if each head is assumed to generate the maximum isometric force of 1 pN [18], the average number of myosin heads involved in the movement of  $V_1$ - and  $V_3$ -coated beads is estimated to be 7 and 6 respectively. Recently, Finer et al. [19] recorded force spikes (about 3 pN) generated by a single myosin molecule using the optical trap technique. This may not be inconsistent with the above assumptions, since our value 1 pN is a time-averaged force during steady actin–myosin sliding.

In Fig. 5 are shown the  $P$ - $V$  curves obtained from five different  $V_1$ -coated beads and from five different  $V_3$ -coated bead. Both the velocity and force (= load) values are expressed relative to their maximum values. The hyper-

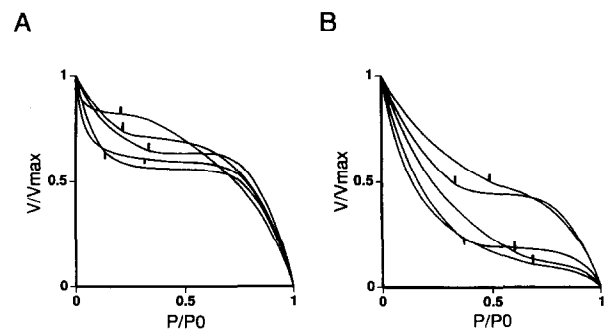


Fig. 5. Differences in shape between the  $P$ - $V$  curves obtained from  $V_1$ -coated beads (A) and those obtained from  $V_3$ -coated beads (B). Velocities and forces are expressed relative to the maximum unloaded shortening velocity ( $V_{\max}$ ) and the maximum isometric force ( $P_0$ ), respectively. In each curve, the critical force above which the curve deviates from the hyperbola is indicated by a short vertical line.

bolic part of the curve in the low force range was found to be much more limited in  $V_1$  than in  $V_3$ . We repeated the hyperbolic fit along regression curves, determined by the non-linear least square method, and extended the force range towards a critical force value, above which deviation from the hyperbola simply increased with further increase of force range. The critical value of force above which the curve deviated from the hyperbola was  $0.24 \pm 0.08 P_0$  ( $n = 5$ ) for the  $V_1$  (Fig. 5A), and  $0.49 \pm 0.15 P_0$  ( $n = 5$ ) for the  $V_3$  (Fig. 5B). The hyperbolic part of the  $P$ - $V$  curves was fitted to the Hill equation:

$$(P + a)(V + b) = (P_0 + a)b$$

where  $V$  is the steady velocity of the bead movement under a constant force  $P$ , and  $a$  and  $b$  are constants. The value of  $a/P_0$ , determining the curvature of  $P$ - $V$  curve, was found to be  $0.21 \pm 0.18$  ( $n = 5$ ) for  $V_3$ . In the case of  $V_1$ , however, the horizontal asymptote of the hyperbolic part of the  $P$ - $V$  curve was above the force axis to result in a negative value of  $b$ . As this renders the Hill equation non-realistic, we corrected the  $P$ - $V$  curve of  $V_1$  in a manner described later.

### 3.4. Possible explanation for the $P$ - $V$ relations obtained on the basis of the Huxley contraction model

Recent careful studies on single skeletal muscle fibers [20] and on cardiac trabeculae [21] have demonstrated that their  $P$ - $V$  curves obviously deviate from the hyperbola in the high force region. Therefore, the purpose of our corrections is to account for the possible cause of the strange shape of  $P$ - $V$  curves in the low force region.

During the ATP-dependent actin-myosin sliding, each myosin head repeats alternate formation and breaking of linkage with actin. In the Huxley contraction model, the probability that an arbitrarily chosen cross bridge is attached is determined by the forward and backward rate constants resulting in a certain value  $0 < p < 1$ . Then, the probability that all the myosin heads interacting with actin

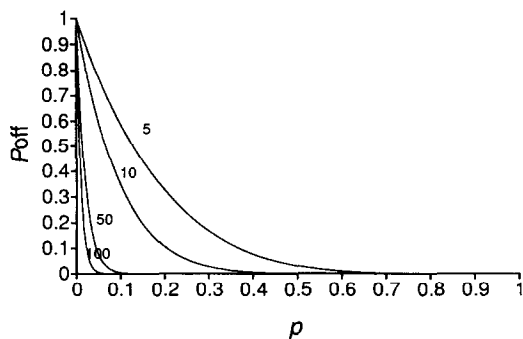


Fig. 6. Dependence of 'off' probability ( $P_{\text{off}}$ ) on the proportion ( $0 < p < 1$ ) of myosin heads attached to actin.

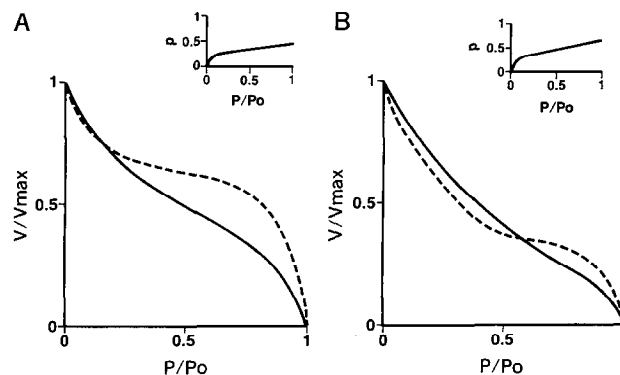


Fig. 7. Corrected  $P$ - $V$  curves (solid lines) for  $V_1$  (A) and for  $V_3$  (B), which are obtained from typical  $P$ - $V$  curves (broken lines) for  $V_1$  (A) and for  $V_3$  (B). The  $p$  vs. load relations for  $V_1$  (A) and for  $V_3$  (B) are also shown (insets).

are in detached state, i.e., 'off' probability ( $P_{\text{off}}$ ) is given by

$$P_{\text{off}} = (1 - p)^N$$

where  $N$  is the number of myosin heads interacting with actin. In Fig. 6, the value of  $P_{\text{off}}$  is plotted as a function of the  $p$  values for various values of  $N$ . It is clear that  $P_{\text{off}}$  is negligibly small for large values of  $N$ , but becomes substantial for small values of  $N$ , especially if the value of  $p$  is sufficiently small. This implies that, in the present experiments in which only a limited number of myosin heads are involved in the actin-myosin sliding,  $P_{\text{off}}$  would be large enough to seriously affect the bead movement.

When all myosin heads are detached from actin for a time period  $\Delta t$ , the bead on cables will be pulled back (or will not go forward under the unloaded condition) by the centrifugal force for a distance  $d$ , which is given by,

$$d = P/f \cdot \Delta t$$

where  $P$  is the centrifugal force (= load), and  $f$  is the friction coefficient of the bead (see Appendix, Eqs. (1), (2) and (3)). Thus, if the number of myosin head involved in the bead movement is extremely small, the bead moves on actin cables with alternate forward and backward (or stoppage) movements. The resulting velocity of bead movement is the average velocity of the zig-zag bead movement, and is considerably smaller than the velocity of bead movement caused by a large number of myosin heads. According to the Huxley contraction model,  $p$  decreases with decreasing external load, reaching a minimum value when the load tends to zero; an idea supported by the stiffness-load relation of single tetanized muscle fibres [22,23].

We estimated the effect of  $P_{\text{off}}$  on the shape of  $P$ - $V$  relation of  $V_1$  and  $V_3$ , based on the experimental data of heat production in isometrically contracting mammalian papillary muscles [24]. The assumptions made are (1) the value of  $p$  is 0.45 for  $V_1$  and 0.6 for  $V_3$  in isometric

condition (velocity = zero), (2)  $p$  decreases in proportion to the external load, reaching 0.04 for  $V_1$  and 0.05 for  $V_3$  under unloaded condition, and (3) the  $p$  versus load relation is straight except for  $P < 0.1P_0$  (inset in Fig. 7). The assumption (3) is based on the fact that the stiffness-load relation tends to be steeper as the load approaches zero [22,23], and is effective in extending the hyperbolic part of the  $P$ - $V$ -curve. The  $p$  values under unloaded condition have also been estimated for the in vitro actin filament sliding on skeletal and smooth muscle myosins to be 0.04–0.05 [25,26], suggesting the validity of our  $p$  values used in the present study.

Fig. 7 shows examples of the correction of  $P$ - $V$  curves of  $V_1$  and  $V_3$ , which are obtained by calculating the velocity  $V$  with  $P_{\text{off}} = 0$  from the measured velocity  $V'$  under various external load (see Appendix, Eqs. (4) and (5)). After the correction, the  $P$ - $V$  curves for  $V_1$  and  $V_3$  were made closer to each other in shape. Especially, the hyperbolic part of the  $P$ - $V$  curve for  $V_1$  was extended to a higher force range up to about  $0.67P_0$ , (Fig. 7A) As a result, the value of  $a/P_0$  for the corrected  $P$ - $V$  curve for  $V_1$  took a positive value (0.29, Fig. 7A) instead of the negative value for the uncorrected  $P$ - $V$  curves (Fig. 4A and 5A). On the other hand, the corrected  $P$ - $V$  curve for  $V_3$  (Fig. 7B) did not differ markedly from the uncorrected ones (Fig. 4B and 5B), except for a slight decrease in the value of  $a/P_0$  (0.18, Fig. 7B). In either case, however, the  $a/P_0$  value for the corrected  $P$ - $V$  curve was close to that obtained in papillary muscle preparation [24].

#### 4. Discussion

In the present experiments, we have succeeded in determining the steady-state  $P$ - $V$  relations of mammalian cardiac myosin isozymes,  $V_1$  and  $V_3$ , using an in vitro assay system in which  $V_1$ -or  $V_3$ -coated polystyrene beads were made to slide on actin cables mounted on the centrifuge microscope [9]. As has been the case in mammalian skeletal muscle myosin [9], the  $P$ - $V$  curves for  $V_1$  and  $V_3$  consisted of hyperbolic part in the low force range and non-hyperbolic part in the high force range (Fig. 4 and Fig. 5). Since the  $P$ - $V$  curve is known to consist of hyperbolic and non-hyperbolic parts in both intact and glycerinated skeletal muscle fibers [20,27,28] and intact cardiac trabeculae [21], our assay system retains basic characteristics of ATP-dependent myofilament sliding. In accordance with this view, it has been shown that the myosin-coated bead surface is covered with well organized myosin filaments, but not with randomly oriented myosin molecules [29]. There may still remain some questions about the assay system. Firstly, the use of *Nitellopsis* actin may have significant influence on the results. However, in addition to the highly conserved primary structure of actin molecules throughout the course of evolution [30], *Nitellopsis* actin can support the sliding movement of myosin obtained from

various tissues at a rate comparable to its ATPase activity [6–8]. Secondly, although the myosin concentration of incubating solution was adjusted for both isozymes, local density of myosin heads might vary not only between two isozymes but also among beads in the same preparation. This heterogeneity could account for the variation in  $P_0$ .

The result that the maximum unloaded velocity of bead movement is much faster for  $V_1$  than for  $V_3$  (Fig. 3, Fig. 4, Fig. 5) indicates, together with the good correlation between the unloaded velocity of myosin-coated beads and the  $\text{Ca}^{2+}$ -activated ATPase activity of myosin samples [7,8], that the rate of cyclic actin-myosin interaction coupled with ATP hydrolysis is much faster for  $V_1$  than for  $V_3$ . This view is consistent with the fact that, in mammalian papillary muscles, the unloaded shortening velocity is much faster in preparations consisting predominantly of  $V_1$  than in preparations consisting predominantly of  $V_3$  [4,5]. On the other hand, the maximum isometric force generated by myosin heads on the bead did not differ significantly between  $V_1$  and  $V_3$ , in agreement with the reports that, in mammalian ventricular trabeculae and papillary muscle, the maximum isometric force per unit cross-sectional area does not differ appreciably between control and hypo or hyperthyroid animals [31,32].

In the present study, we have presented a possible explanation for the  $P$ - $V$  relations of myosin-coated beads moving on actin cables within the framework of the Huxley contraction model [10]. In the above explanation, the limited hyperbolic part of the  $P$ - $V$  curves, especially that for  $V_1$  arises from the substantial value of "off" probability ( $P_{\text{off}}$ ) when the number of myosin heads interacting with actin is extremely small. By calculating the velocity values with  $P_{\text{off}}$  for various loads, we could correct the  $P$ - $V$  curves for both  $V_1$  and  $V_3$  (Fig. 4 and Fig. 5) to obtain the corrected  $P$ - $V$  curves (Fig. 7). The curves resemble the  $P$ - $V$  curves of papillary muscle preparation from rabbit hearts with and without pressure overload [24] with respect to their shapes. This indicates that the difference in  $P$ - $V$  curves they observed actually reflects the change in myosin isozyme composition of the preparations. The validity of the idea of  $P_{\text{off}}$  as the cause of the marked deviation from the hyperbola of the  $P$ - $V$  relations may be supported not only by the present study, but also by the previous report that the deviation from the hyperbola of the  $P$ - $V$  relations in the ATP-dependent movement of beads coated with skeletal muscle myosin on actin cables [9] is more marked with beads generating small  $P_0$  than with those generating large  $P_0$ .

#### Acknowledgements

This study was supported in part by the grant from Fukuda Memorial Fund for the Biomedical Technology, the Vehicle Racing Commemorative Foundation, and Japan Heart Foundation Research Grant.

## Appendix A

### Movement of a myosin-coated bead on actin cables under constant centrifugal forces

The constant velocity of movement of a myosin-coated bead on actin cables under a constant centrifugal force can be expressed by the equation,

$$M(d^2x/dt^2) = -f(dx/dt) + P \quad (1)$$

where  $M$  is bead mass,  $x$  is bead displacement,  $f$  is friction coefficient of a bead ( $= 6 \cdot \pi \cdot \eta \cdot r$ , where  $r$  is bead radius and  $\eta$  is viscosity of the surrounding medium), and  $P$  is external load produced by a constant centrifugal force. As  $r = 1.4 \mu\text{m}$  and  $\eta = 0.01$  poise (viscosity of water),  $f$  is calculated to be  $2.6 \cdot 10^{-8} \text{ N s m}^{-1}$ . Since  $M$  is very small ( $1.5 \cdot 10^{-14} \text{ kg}$ ), Eq. (1) can be simplified to,

$$fV = P \quad (2)$$

where  $V (= dx/dt)$  is velocity of bead movement. Thus, if all myosin heads are detached from actin cables for a time period  $t$ , the bead moves backward for a distance  $x$ , which is given by,

$$x = (P/f)t. \quad (3)$$

### Correction of the observed velocity values based on "off" probability

The velocity of bead movement  $V$  with zero "off" probability ( $P_{\text{off}} = 0$ ) can be calculated from the observed velocity  $V'$  by the following equation,

$$V' = V(1 - (1 - p)^N) - (P/f)(1 - p)^N. \quad (4)$$

The above equation is also written as:

$$V = (V' + (P/f)(1 - p)^N) / (1 - (1 - p)^N). \quad (5)$$

In this simulation,  $N$  was set at 10 for both  $V_1$  and  $V_3$  in order to evaluate only the effect of the difference in  $p$  between two isozymes.

## References

[1] Hoh, J.F.Y., MacGrath, P.A. and Hale, P.T. (1977) *J. Mol. Cell. Cardiol.* 10, 1053–1076.

- [2] Izumo, S., Lompré, A.M., Matsuoka, R., Koren, G., Schwartz, K., Nadal-Ginard, B. and Mahdavi, V. (1987) *J. Clin. Invest.* 79, 970–977.
- [3] Lompré, A.M., Nadal-Ginard, B. and Mahdavi, V. (1984) *J. Biol. Chem.* 259, 6437–6446.
- [4] Cappelli, V., Bottinelli, R., Poggesi, C., Moggio, R. and Reggiani, C. (1989) *Circ. Res.* 65, 446–457.
- [5] Schwartz, K., Lecarpentier, Y., Martin, J.L., Lompré, A.M., Mercadier, J.J. and Swynghedauw, B. (1981) *J. Mol. Cell. Cardiol.* 13, 1071–1075.
- [6] Sheetz, M.P. and Spudich, J.A. (1984) *J. Cell. Biol.* 99, 1867–1871.
- [7] Sugiura, S., Yamashita, H., Serizawa, T., Iizuka, M., Shimmen, T. and Sugimoto, T. (1992) *Pflügers Arch.* 421, 32–36.
- [8] Yamashita, H., Sugiura, S., Serizawa, T., Sugimoto, T., Iizuka, M., Katayama, E. and Shimmen, T. (1992) *Am. J. Physiol.* 263, H464–H472.
- [9] Oiwa, K., Chaen, S., Kamitsubo, E., Shimmen, T. and Sugi, H. (1990) *Proc. Natl. Acad. Sci. USA* 87, 7893–7897.
- [10] Huxley, A.F. (1957) *Prog. Biophys. Biophys. Chem.* 7, 255–318.
- [11] Katz, A.M., Repke, D.I. and Rubin, B.B. (1966) *Circ. Res.* 19, 611–621.
- [12] Martin, A.F., Pagani, E.D. and Solaro, R.J. (1982) *Circ. Res.* 50, 117–124.
- [13] Yazaki, Y. and Raben, M.S. (1974) *Circ. Res.* 35, 15–23.
- [14] Lowry, O.H., Rosebrough, N.J., Farr, A.L. and Randall, R.J. (1951) *J. Biol. Chem.* 193, 265–275.
- [15] Shimmen, T. and Yano, M. (1984) *Protoplasma* 121, 132–137.
- [16] Kamitsubo, E., Ohashi, Y. and Kikuyama, M. (1989) *Protoplasma* 152, 148–155.
- [17] Yazaki, Y. and Raben, M.S. (1975) *Circ. Res.* 36, 208–215.
- [18] Hill, T.L. (1974) *Progr. Biophys. Mol. Biol.* 28, 267–340.
- [19] Finer, J.T., Simmons, R.M. and Spudich, J.A. (1994) *Nature* 368, 113–119.
- [20] Edman, K.P. (1988) *J. Physiol.* 404, 301–321.
- [21] De Tombe, P.P. and Ter Keurs, H.E.D.J. (1990) *Circ. Res.* 66, 1239–1254.
- [22] Julian, F.J. and Sollins, M.R. (1975) *J. Gen. Physiol.* 66, 287–302.
- [23] Sugi, H. and Tsuchiya, T. (1981) *J. Physiol.* 319, 239–252.
- [24] Alpert, N.R. and Mulieri, L.A. (1983) in *Perspectives in cardiovascular research* (Alpert, N.R., ed.), Vol. 7, pp. 619–630, Raven Press, New York.
- [25] Uyeda, T.P.Q., Kron, S.J. and Spudich, J.A. (1990) *J. Mol. Biol.* 214, 699–710.
- [26] Harris, D.E. and Warshaw D.M. (1993) *J. Biol. Chem.* 268, 14764–14768.
- [27] Iwamoto, H., Sugaya, R. and Sugi, H. (1990) *J. Physiol.* 422, 185–202.
- [28] Sugi, H., Kobayashi, T., Gross, T., Noguchi, K., Karr, T. and Harrington, W.F. (1992) *Proc. Natl. Acad. Sci. USA* 89, 6134–6137.
- [29] Takahashi, I., Oiwa, K., Kawakami, T., Tanaka, H. and Sugi, H. (1993) *J. Electron. Microsc.* 42, 334–337.
- [30] Korn, E.D. (1982) *Physiol. Rev.* 62, 672–737.
- [31] Ebrecht, G., Rupp, H., and Jacob, R. (1982) *Basic Res. Cardiol.* 77, 220–234.
- [32] Shibata, T., Hunter, W.C. and Sagawa, K. (1987) *Circ. Res.* 60, 770–779.